

SHORT COMMUNICATION

---

GRAIN COUPLING CONTRIBUTION TO SUPERCONDUCTIVITY IN CERAMIC YBCO BY MAGNETIC MEASUREMENTS

N.SPARVIERI

Selenia SPA, Research Dep. Via Tiburtina Km 12.4 , 00131 Rome (Italy)

Received October 31, 1990; accepted November 5, 1990

ABSTRACT

Using a Vibrating Sample Magnetometer (VSM), the magnetization of sintered YBCO prepared with flame spraying (pyrolysis) and annealed in an ozone atmosphere, has been studied. Measurements of the initial magnetization curves performed at 67 K in zero field cooling, show a small peak at about 20 Oer attributed to weak links between superconducting grains. Fine powdering (crushing and sieving) of the ceramic sample allow one to distinguish the grain coupling effects. The differential magnetization curve  $\Delta M/M = [M_{\text{pellet}}(H) - M_{\text{powdered}}(H)]/M_{\text{powdered}}(H)$  shows a strong peak at low fields attributed to the grain coupling contribution to superconductivity.

Moreover the behavior of the hysteresis loop area vs maximum applied field is presented which clearly shows three different penetration flux regimes confirming the initial penetration of the grain boundaries followed by the penetration inside them.

INTRODUCTION

Sintered high  $T_c$  superconductors generally have a very low critical current density  $J_c$  that is limited by the weak coupling existing between the superconducting grains of the material. The application of a magnetic field further reduced the critical current densities to values too low to be of practical use in the majority of applications. From direct measurements of  $J_c$  of individual grain boundaries (GB) in YBCO [1] it is known that there is a poor superconducting coupling across the GB; in the bicrystal case it was shown that  $J_c$  falls rapidly with increasing misorientation angle. Additionally, work on the temperature and magnetic field dependence of

the GB critical current indicates that the boundaries behave as superconductor-normal-superconductor (SNS) weak links [2]. These results support the suggestion that the GB in ceramic high  $T_c$  superconductors can be treated as Josephson junctions in which there is a reduced superconducting pair potential. This is probably due to the structural disorder at the GB or it could be a consequence of the short coherence lengths, smaller than the GB length (in YBCO  $\xi_{ab} \sim 15 \text{ \AA}$ ,  $\xi_c \sim 3 \text{ \AA}$ ). The complex of this information forms a picture of the material in terms of a distribution of critical current values throughout the microstructure; the actual transport critical current is determined by the topological interconnectivity of the paths, as in a percolation problem. There are a variety of such paths each with a different value of critical current density.

Among the limiting factors for grain coupling there is, of course, the processing. In the  $Y_2O_3$ -BaO-CuO phase diagram there is a low melting eutectic for compositions rich in CuO and BaO with respect to the stoichiometry of the 1-2-3 phase [3]. This is a liquid eutectic (melting temperature  $890^\circ\text{C}$  in air) which promotes densification but it produces an insulating GB phase. It is probably due to reaction with carbon dioxide gas to form an oxycarbonate liquid [4]. This is supported by EELS spectroscopy of the liquid phase in GB in air sintered materials which indicates the presence of carbon. Also Auger analysis performed on the surface of *in situ* fractured pellets showed a high carbon concentration localized on the GB [5]. Carbonate like chemical bonding at GB of YBCO can also exist for incomplete decomposition of  $BaCO_3$  (if used as starting material)[6].

Magnetic investigation of high  $T_c$  pellets puts directly in evidence their granular nature *i.e.* allow a separation between the grain coupling contribution and the grain contribution to superconductivity. The main result of this technique is the definition of a hierarchy of critical fields depending on the strength of the grain coupling. Such an investigation neglects the microscale aspects of the material (mechanisms of superconductivity, crystal structure etc) but it uses the mesoscale approach typical for granular media.

In this paper the magnetic properties of sintered pellets have been analyzed using a VSM technique. The main steps of the fabrication process are described and the experimental results are reported which quite clearly show the grain coupling contribution to the magnetic behavior.

## SAMPLE FABRICATION

Samples are fabricated by the flame spraying (pyrolysis) method. The main steps are:

- 1) drying separately of the industrial grade powders of  $BaCO_3$ , CuO,  $Y_2O_3$ .
- 2) add slowly 65% concentrated  $HNO_3$ , avoiding clots, to obtain nitrate solutions with an excess of nitric acid

- 3) put together all the three liquids and add citric acid
- 4) add slowly, 25% concentrated,  $\text{NH}_4\text{OH}$  until the pH reaches the value of about 6.8
- 5) take a fraction of reacted liquid and warm up until flame spraying begins
- 6) fill an alumina crucible with the ultra fine reacted powder (about 100 nm) and heat at 950 °C for 10 h in an ozone enriched atmosphere (cooling rate 50 °C/h)
- 7) press at about 10 K Bar
- 8) heat again like step 6).

As final result is obtained a single phase material tested by its neutron diffraction pattern and with density of 5.5-5.9 gm  $\text{cm}^{-3}$ . Further details on the preparation procedure and physical characterization are reported elsewhere [7-9].

## RESULTS

In Fig. 1 the first magnetization curve (surface shielding currents) at 67 K in zero field cooling on a spherical shaped sample is depicted.

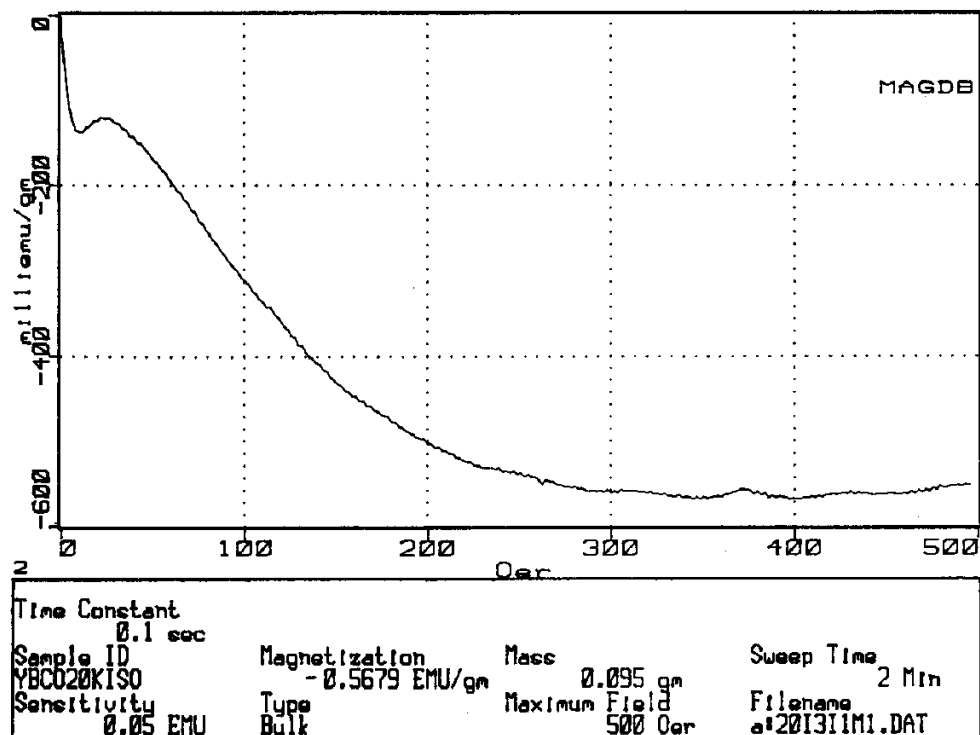


Fig. 1. First magnetization curve at 67K in zero field cooling on a spherical shaped sample.

The increase of the applied magnetic field will increase the shielding currents on the sample surface, until it overcomes the critical current of the weakest link between grains, with magnetic flux partial penetration. The subsequent decay of the superconducting currents (close to 12 Oer in Fig.1) generates an entrapment of magnetic flux quanta in the intergrain regions (in such a way that the lower critical field  $H_{C1}^G$  is determined by the grain coupling). Further increase of the magnetic field will increase the entrapment of magnetic flux until  $H_{C2}^G$  is reached. Above this value (about 25 Oer in Fig. 1) the magnetic field penetrates completely in the intergranular regions and the grains will be decoupled. This is in accord with critical current density measurements in magnetic fields [10]. Further increase of the magnetic field will increase the shielding currents on the grain surface until it exceeds the true lower critical field  $H_{C1}$  of the material and the penetration inside the grain starts.

In Fig.2 is shown the first magnetization curve on the same sample after fine powdering *i.e.* after mechanical destruction of the grain coupling. The reduction of the signal is due to the large amount of defects induced in the crushing process. Figure 3 shows the differential magnetization curve  $\Delta M/M = [M_{\text{pellet}}(H) - M_{\text{powdered}}(H)] / M_{\text{powdered}}(H)$  proportional to the grain coupling itself.

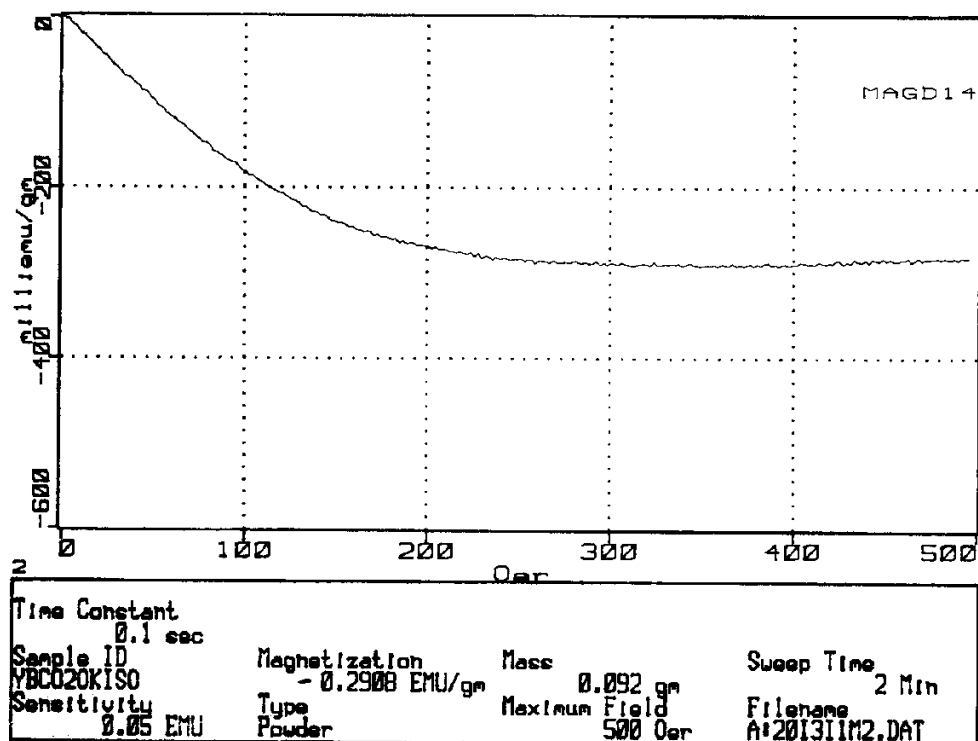


Fig.2. First magnetization curve on the same sample at 67 K after crushing and sieving (mechanical destruction of the grain coupling).

$\Delta M/M$ 

## DIFFERENTIAL MAGNETIZATION

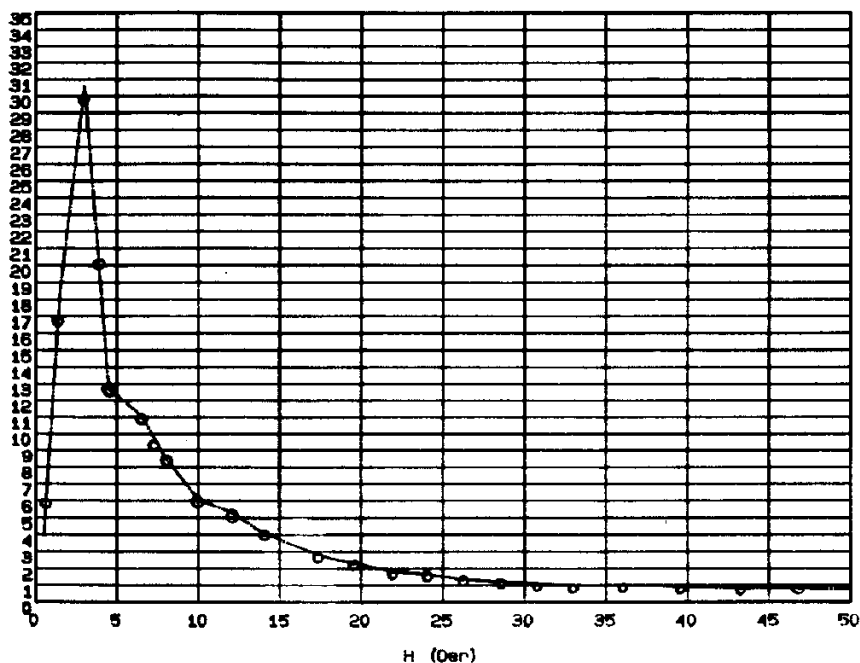


Fig. 3. Differential magnetization curve  $\Delta M/M = [M_{\text{pellet}}(H) - M_{\text{powdered}}(H)] / M_{\text{powdered}}(H)$

Another complementary way to observe the grain coupling contribution is by the hysteresis loop area behavior vs. maximum applied field. This relationship gives information on the total flux penetration in the sample. Of course the total flux trapped has two contributions: the first is due to the structural defects which contribute as pinning centers with their different activation energies, and the second is the physical effect of weak link destruction. The first contribution is like a uniform 'background' always present both in the weak link destruction and in grain penetration. It is directly related to the preparation of the sample. At small fields the system is a bulk superconductor and there is no trapped flux and, consequently, zero area until  $H_{C1}^G$  is reached. After that magnetic flux partial penetration in the weak link partial penetration in the weak link generates hysteresis until  $H_{C2}^G$ .

The log-log plot in Fig.4 of the hysteresis loop area shows the existence of three different regimes: a) weak link destruction between  $H_{C1}^G$  and  $H_{C2}^G$  (about 3 to about 7 Oer); b) a second regime (from 7 to about 150 Oer) due to flux pinning in structural defects not masked by other physical effects and finally c) a strong hysteretic regime associated with a massive penetration of the magnetic flux into the grains which starts at about 150 Oer ( $H_{C1}$  of the sample). This latter value can be related with the linearity displacement value of the first magnetization curve of Fig.1.

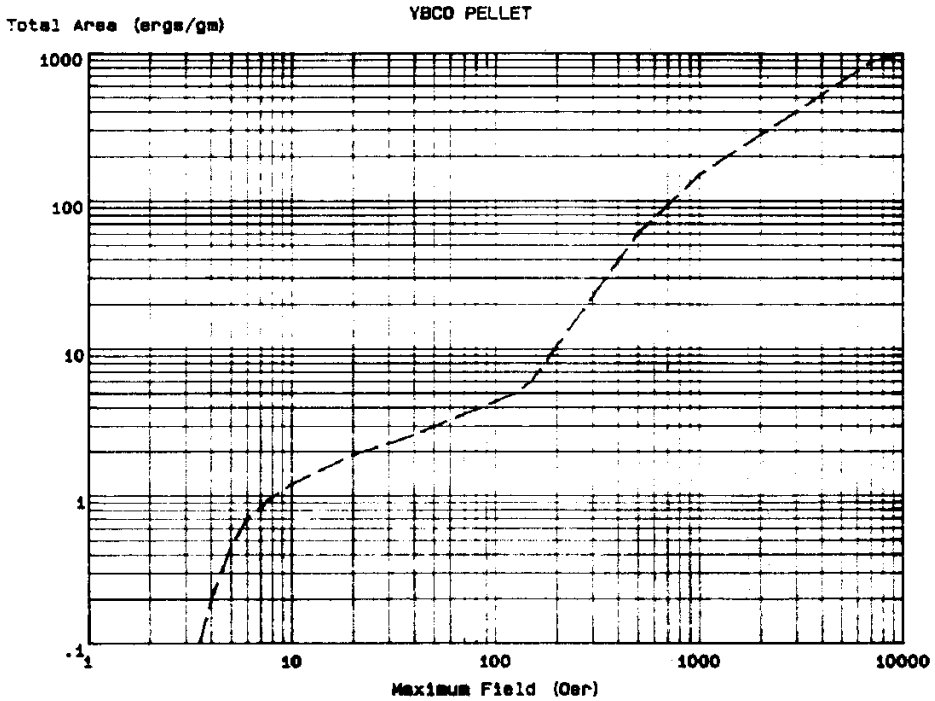


Fig.4. log-log plot of the hysteresis loop area behavior.

## CONCLUSIONS

The measurements performed by VSM show the grain coupling contribution at superconductivity in YBCO samples obtained by the flame spraying (pyrolysis) fabrication method. Indeed, experimental data can be related with data from complementary techniques giving a more detailed picture of the granular superconductor behavior. In particular  $J_c$  vs.  $H$  measurements [10] give a breakdown field in accord with the  $H_{C2}^G$  value reported in this paper.

Moreover magnetic torque measurements [11] show the three penetration field regimes in accord with the hysteresis loop area measurements presented.

The weak link decay law in  $\Delta M/M$  can be utilized as a support for modeling of a random 3D structure of Josephson junctions.

## REFERENCES

- 1 P.Chaudhari, J.Mannhart, D.Dimos, C.C.Tsuei, J.Chi, M.M.Oprysko and M.Scheuermann  
Phys. Rev. Lett., **60**, (1988)1653.
- 2 K.K.Likharev, Rev. Mod. Phys. **51** [1] (1979)101.
- 3 D.L.Kaiser, F.Holtzberg, B.A.Scott and T.R.McGuire, Appl. Phys. Lett. **51**[3](1987)1040.
- 4 R.S. Roth, C.J.Rawn, F.Beech, J.D.Whitler and J.O.Anderson in M.F.Yan (ed.), Ceramic Superconductors ; Am. Ceram. Soc., Westerville, OH, 1988. p p. 13-27
- 5 L.Zhang , J. Am. Ceram. Soc., **72**(1989) 1997.
- 6 D.R.Clark, T.M.Shaw and D.Dimos J. Am. Ceram. Soc. **72**[7] (1989)1103
- 7 F.Celani, L.Liberatori, R.Messi, S.Pace, A.Saggese and N.Sparvieri, Proceedings of the International Symposium on the electronic structure of high Tc superconductors, Pergamon press 1988. Rome 5-7 Oct. 1988 Accademia dei Lincei.
- 8 F.Celani, R.Messi, S.Pace and N.Sparvieri, Il Nuovo Saggiatore, **4**(1988)7
- 9 N.Sparvieri, F.Celani, W.I.F.David, C.Giovannella, R.Messi, V.Merlo, S.Pace and A.Saggese Vuoto Vol XVIII N.3 Luglio-Settembre 1988.
- 10 G.Paternò , Physica C, **153**(1988)1341
- 11 F.Celani, L.Fruchter, C.Giovannella, R.Messi, S.Pace, A.Saggese and N.Sparvieri, IEEE Transactions Mag. Vol. 25, No. 2, March 1989.